

## Denhaminols A–H, Dihydro- $\beta$ -agarofurans from the Endemic Australian Rainforest Plant *Denhamia celastroides*

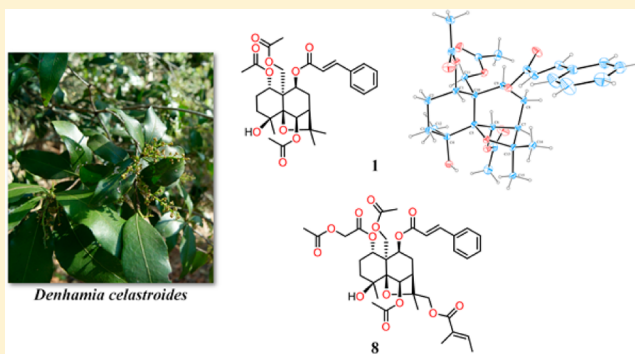
Claire Levrier,<sup>†,‡</sup> Martin C. Sadowski,<sup>‡</sup> Colleen C. Nelson,<sup>‡</sup> Peter C. Healy,<sup>†</sup> and Rohan A. Davis<sup>\*,†</sup>

<sup>†</sup>Eskitis Institute for Drug Discovery, Griffith University, Brisbane, QLD 4111, Australia

<sup>‡</sup>Australian Prostate Cancer Research Centre—Queensland, Institute of Health and Biomedical Innovation, Queensland University of Technology, Princess Alexandra Hospital, Translational Research Institute, Brisbane, QLD 4102, Australia

### S Supporting Information

**ABSTRACT:** Eight new dihydro- $\beta$ -agarofurans, denhaminols A–H (1–8), were isolated from the leaves of the Australian rainforest tree *Denhamia celastroides*. The chemical structures of 1–8 were elucidated following analysis of 1D/2D NMR and MS data. The absolute configuration of denhaminol A (1) was determined by single-crystal X-ray crystallography. All compounds were evaluated for cytotoxic activity against the human prostate cancer cell line LNCaP, using live-cell imaging and metabolic assays. Denhaminols A (1) and G (7) were also tested for their effects on the lipid content of LNCaP cells. This is the first report of secondary metabolites from *D. celastroides*.



Due to its evolutionary isolation, Australia is considered a megadiverse country.<sup>1</sup> The concept of megadiversity is defined as “the total number of species in a country and the degree of endemism at the species level and at higher taxonomic levels.”<sup>2</sup> A total of 17 megadiverse countries have been identified, and Australia is ranked fifth in terms of the number of endemic vascular plant species.<sup>2</sup> Australia’s floral biodiversity can be explained by the variety of terrestrial ecosystems inclusive of arid, semiarid, shrub land, temperate grassland, and tropical and subtropical rainforest.<sup>2</sup> *Denhamia* is an Australian endemic genus, consisting of seven species, which belongs to the Celastraceae plant family.<sup>3</sup> This pantropical family contains 87 genera and 1168 species,<sup>4</sup> with 14 genera and 34 species found in Australia.<sup>5</sup> *Denhamia celastroides*, also known as Orange Box Thorn, grows as a shrub or small tree up to 7 m high.<sup>3</sup> This tree is native to Queensland and northern New South Wales and occurs in most types of rainforest and margins within wet sclerophyll forest.<sup>3</sup> To date, only one phytochemical study has been reported on the genus *Denhamia*, with chemical investigations of the bark of *Denhamia pittosporoides* affording the highly cytotoxic quino-nemethide triterpene pristimerin.<sup>6</sup> Furthermore, plants of the Celastraceae family are known to produce different classes of compounds, including diterpenes,<sup>7</sup> triterpenes,<sup>8</sup> sesquiterpenes,<sup>9</sup> and alkaloids.<sup>7,9</sup> Most of the sesquiterpenes isolated from this plant family are dihydro- $\beta$ -agarofurans, which are based on a 5,11-epoxy-5 $\beta$ ,10 $\alpha$ -eudesman-4-(14)-ene skeleton.<sup>10</sup> These compounds can be oxygenated in numerous positions and display a variety of substituents, such as *O*-acetyl, *O*-benzoyl, and nicotinoyl rings.<sup>7</sup> This structure class is so widespread in this plant family that they are considered as

chemotaxonomic indicators of Celastraceae.<sup>11</sup> This compound class has been shown to exhibit a broad range of biological activities, such as insecticidal,<sup>12</sup> cytotoxicity,<sup>13</sup> and suppression of multidrug resistance (MDR) in cancer cells.<sup>14</sup>

*D. celastroides* was selected for this study due to the propensity of Celastraceae species to produce bioactive and new compounds and the fact that no phytochemical studies had been previously undertaken on this endemic Australian species.

This report describes the isolation and structure elucidation of eight new dihydro- $\beta$ -agarofurans, denhaminols A–H (1–8), from the leaves of *D. celastroides*. Furthermore, the in vitro cytotoxicity evaluation for all compounds toward LNCaP prostate cancer cells is also reported, as well as the effect of denhaminols A (1) and G (7) on the cellular content of phospholipids and neutral lipids.

### RESULTS AND DISCUSSION

The major metabolite, compound 1, was isolated as colorless needles. The molecular formula was determined to be C<sub>30</sub>H<sub>38</sub>O<sub>10</sub>, as indicated by the (+)-HRESIMS and NMR data. The IR spectrum of 1 showed absorption bands consistent with a hydroxy group (3544 cm<sup>−1</sup>) and ester groups (1739 cm<sup>−1</sup>). The <sup>1</sup>H NMR spectrum of 1 (Table 1 and Experimental Section) showed three tertiary methyl signals at  $\delta_H$  1.52, 1.54, and 1.32, three *O*-acetyl signals at  $\delta_H$  1.81, 2.10, and 2.25, four sets of methylene protons at  $\delta_H$  1.45–1.92, 1.71–1.90, 2.17–2.47, and 4.45–4.63, 11 methine protons at  $\delta_H$  2.14, 5.21, 5.43, 6.06, 6.37, 7.40 (2H), 7.41, 7.54 (2H), and 7.69, and a hydroxy

Received: September 25, 2014

Published: January 12, 2015

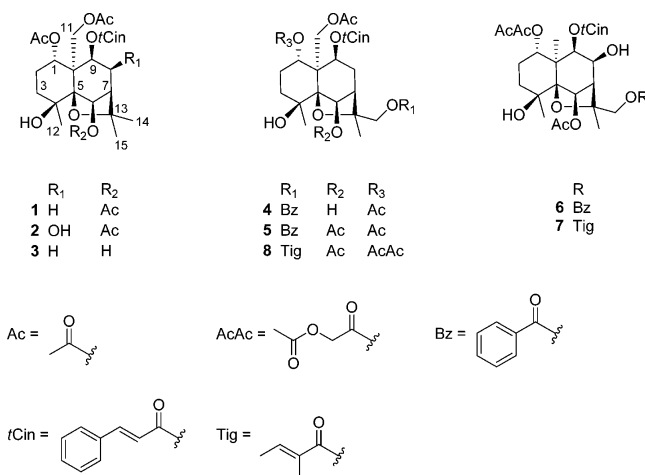


**Table 1.**  $^1\text{H}$  NMR Spectroscopic Data of Denhaminols A–D (1–4)<sup>a</sup>

position	1	2	3	4
$\delta_{\text{H}}$ (mult. $J$ in Hz)	$\delta_{\text{H}}$ (mult. $J$ in Hz)	$\delta_{\text{H}}$ (mult. $J$ in Hz)	$\delta_{\text{H}}$ (mult. $J$ in Hz)	$\delta_{\text{H}}$ (mult. $J$ in Hz)
1	5.43, dd (12.2, 4.2)	5.49, dd (12.6, 4.1)	5.46, dd (12.6, 4.1)	5.42, dd (12.2, 4.1)
2	1.45, m	1.43, m	1.44, m	1.43, m
	1.92, m	1.97, m	1.95, m	1.95, m
3	1.71, m	1.74, m	1.73, m	1.76, m
	1.90, m	1.93, m	1.94, m	1.97, m
OH-4	2.81, s	<sup>b</sup>	<sup>b</sup>	<sup>b</sup>
6	6.06, s	5.90, s	4.73, d (5.3)	4.81, d (5.5)
OH-6			5.12, d (5.3)	5.26, d (5.5)
7	2.14, br dd (3.7, 3.0)	2.40, br d (3.3)	2.24, br dd (3.6, 2.8)	2.51, br dd (3.9, 2.9)
8	2.17, dd (16.0, 3.0)	4.57, dd (6.4, 3.3)	2.14, dd (15.8, 2.8)	2.12, br dd (16.4, 2.9)
	2.47, ddd (16.0, 7.2, 3.7)		2.27, ddd (15.8, 7.1, 3.6)	2.33, ddd (16.4, 7.5, 3.9)
OH-8		<sup>b</sup>		
9	5.21, d (7.2)	5.37, d (6.4)	5.19, d (7.1)	5.30, d (7.5)
11	4.45, d (12.5)	4.41, d (12.5)	4.50, d (12.3)	4.54, d (12.5)
	4.63, d (12.5)	4.62, d (12.5)	4.55, d (12.3)	4.57, d (12.5)
12	1.32, s	1.30, s	1.60, s	1.63, s
14	1.54, s	1.54, s	1.58, s	4.73, d (11.0)
				4.93, d (11.0)
15	1.52, s	1.68, s	1.53, s	1.75, s

<sup>a</sup>Spectra recorded at 600 MHz in  $\text{CDCl}_3$  at 30 °C. For signals corresponding to ester groups and other substituents see the Experimental Section. <sup>b</sup>Not observed.

group signal at  $\delta_{\text{H}}$  2.81. Analysis of the COSY spectrum, in combination with the  $^1\text{H}$ – $^1\text{H}$  coupling constants, identified two spin systems. The first system contained the proton at  $\delta_{\text{H}}$  5.43 (H-1) and two sets of methylene protons [ $\delta_{\text{H}}$  1.45 m (H-2a), 1.92 m (H-2b), 1.71 m (H-3a), 1.91 m (H-3b)]. The second spin system was located between the methine protons at  $\delta_{\text{H}}$  2.14 (H-7) and 5.21 (H-9) and the methylene protons (H-8) resonating at  $\delta_{\text{H}}$  2.17 and 2.47. Two angular methyl groups ( $\delta_{\text{H}}$  1.52 and 1.54) showed HMBC correlations (Figure 1A) to the same quaternary carbon at  $\delta_{\text{C}}$  84.2 and to the carbon bearing the proton at  $\delta_{\text{H}}$  2.14 (H-7). The angular methyl at  $\delta_{\text{H}}$  1.32 ( $\text{CH}_3$ -12) was attached to a downfield carbon at  $\delta_{\text{C}}$  70.1

**Table 2.**  $^1\text{H}$  NMR Spectroscopic Data of Denhaminols E–H (5–8)<sup>a</sup>

position	5	6	7	8
$\delta_{\text{H}}$ (mult. $J$ in Hz)	$\delta_{\text{H}}$ (mult. $J$ in Hz)	$\delta_{\text{H}}$ (mult. $J$ in Hz)	$\delta_{\text{H}}$ (mult. $J$ in Hz)	$\delta_{\text{H}}$ (mult. $J$ in Hz)
1	5.41, dd (12.6, 4.1)	5.40, dd (11.7, 4.3)	5.38, dd (11.6, 4.2)	5.49, dd (12.4, 4.3)
2	1.43, m	1.50, m	1.52, m	1.44, m
	1.95, m	1.93, m	1.93, m	1.92, m
3	1.75, m	1.71, m	1.70, m	1.73, m
	1.97, m	1.88, m	1.89, m	1.93, m
OH-4	<sup>b</sup>	<sup>b</sup>	2.73, br s	<sup>b</sup>
6	6.16, s	5.43, s	5.40, s	6.12, s
7	2.42, br dd (3.3, 2.3)	2.67, br d (3.2)	2.61, br d (3.2)	2.34, br dd (3.6, 2.6)
8	2.23, dd (16.3, 2.3)	4.55, dd (6.4, 3.2)	4.52, dd (6.4, 3.2)	2.18, dd (16.2, 2.6)
	2.56, ddd (16.3, 7.3, 3.3)			2.51, ddd (16.2, 7.1, 3.6)
OH-8		<sup>b</sup>	2.55, br s	
9	5.33, d (7.3)	5.13, d (6.4)	5.12, d (6.4)	5.27, d (7.1)
11	4.66, d (12.5)	1.38, s	1.36, s	4.41, d (12.9)
	4.47, d (12.5)			4.62, d (12.9)
12	1.35, s	1.33, s	1.34, s	1.34, s
14	4.69, d (11.0)	4.93, m	4.71, d (11.7)	4.49, d (11.1)
	4.93, d (11.0)	4.93, m	4.76, d (11.7)	4.71, d (11.1)
15	1.69, s	1.69, s	1.60, s	1.60, s

<sup>a</sup>Spectra recorded at 600 MHz in  $\text{CDCl}_3$  at 30 °C. For signals corresponding to ester groups and other substituents see Experimental Section. <sup>b</sup>Not observed.

**Table 3.**  $^{13}\text{C}$  NMR Spectroscopic Data of Denhaminols A–H (1–8)<sup>a</sup>

position	1	2	3	4	5	6	7	8
$\delta_{\text{C}}$	$\delta_{\text{C}}$	$\delta_{\text{C}}$	$\delta_{\text{C}}$	$\delta_{\text{C}}$	$\delta_{\text{C}}$	$\delta_{\text{C}}$	$\delta_{\text{C}}$	$\delta_{\text{C}}$
1	71.9	72.0	71.7	71.5	71.8	73.5	73.5	73.0
2	23.8	23.8	23.8	24.2	23.8	23.3	23.0	23.8
3	38.2	38.2	37.0	37.1	38.0	38.4	38.0	38.0
4	70.1	70.2	72.9	72.9	70.8	70.6	70.7	70.0
5	91.3	90.9	91.1	92.0	92.9	91.9	92.0	92.0
6	78.3	76.3	78.8	78.5	77.7	77.3	77.0	77.7
7	49.0	54.8	49.9	49.0	48.7	54.7	54.4	48.0
8	34.5	71.7	34.1	34.0	34.0	69.9	69.9	34.3
9	68.8	71.2	68.4	67.8	68.4	74.4	74.2	68.4
10	54.0	52.6	52.9	53.0	55.4	49.9	49.8	54.0
11	65.1	64.4	64.7	64.9	65.1	19.6	19.8	64.9
12	23.7	23.6	23.2	23.4	23.8	24.0	23.9	23.9
13	84.2	84.6	84.6	84.8	85.5	85.0	85.5	84.0
14	29.5	30.3	30.0	69.8	69.1	69.4	68.9	68.7
15	25.6	26.1	26.4	25.2	24.4	24.3	24.4	24.4

<sup>a</sup>Spectra recorded at 150 MHz in  $\text{CDCl}_3$  at 30 °C. For signals corresponding to ester groups and other substituents see Experimental Section.

( $\text{CH}_3$ -12/C-4 HMBC correlation), bearing a hydroxy group. This angular methyl also exhibited HMBC correlations to the carbons resonating at  $\delta_{\text{C}}$  38.2 (C-3) and 91.3 (C-5). Downfield chemical shifts of protons at  $\delta_{\text{H}}$  5.43 (H-1), 5.21 (H-9), and 6.06 (H-6) were assigned to methine protons geminal to ester groups. The *O*-acetyl signals at  $\delta_{\text{H}}$  1.81 (OAc-1) and 2.10 (OAc-6) showed long-range HMBC correlations to C-1 and C-

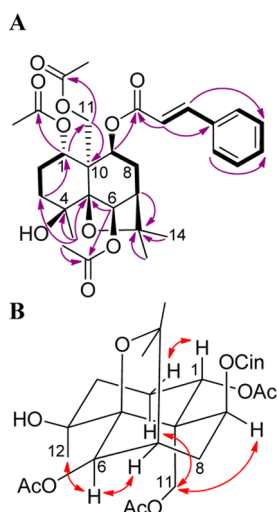


**Figure 1.** Selected (A) HMBC ( $\rightarrow$ ), COSY (bold line), and (B) NOESY ( $\leftrightarrow$ ) correlations of denhaminol A (**1**).

6, respectively. Similarly, the set of methylene protons resonating at  $\delta_{\text{H}}$  4.45 and 4.63 (H-11) were positioned on a carbon bearing a primary *O*-acetyl ( $\delta_{\text{H}}$  2.25). This set of oxygenated methylenes, protons from both spin systems, and the angular methyl showed HMBC correlations to the quaternary carbons at  $\delta_{\text{C}}$  91.3 (C-5) and 54.0 (C-10). These data established that **1** contained a dihydro- $\beta$ -agarofuran scaffold. An aromatic system ( $\delta_{\text{H}}$  7.40, 7.41, and 7.54;  $\delta_{\text{C}}$  128.2, 128.9, 130.8, and 134.2) was attached to two *trans*-olefinic protons at  $\delta_{\text{H}}$  6.37 and 7.69 (each 1H, d,  $J = 15.9$  Hz) by HMBC and COSY correlations. An ester group (carbonyl at  $\delta_{\text{C}}$  165.5) was linked to this (*E*)-2-phenylethenyl moiety to form a *trans*-cinnamoyl moiety.<sup>15</sup> An HMBC correlation between the downfield methine proton at  $\delta_{\text{H}}$  5.21 (H-9) and the carbonyl ( $\delta_{\text{C}}$  165.5) allowed the *trans*-cinnamoyl moiety to be positioned at C-9. The relative configuration of **1** was determined following analysis of the NOESY experimental data (Figure 1B). The  $\alpha$ -orientation of H-6 was established since NOE correlations were observed to H-7 as well as CH<sub>3</sub>-12, which always has an  $\alpha$ -orientation in dihydro- $\beta$ -agarofurans.<sup>10</sup> The NOE cross-peak between H-9 and the signals of H-11 supported the  $\alpha$ -orientation for H-9. The  $\alpha$ -orientation of one of the methylene signals for H-2 ( $\delta_{\text{H}}$  1.45) was determined by the NOE correlation to the methylene proton, H-11 ( $\delta_{\text{H}}$  4.45). A strong NOE correlation between H-1 and the second methylene signal for H-2 ( $\delta_{\text{H}}$  1.92) allowed a  $\beta$ -orientation to be assigned to H-1. This was in good agreement with a number of studies that have shown that in dihydro- $\beta$ -agarofurans H-1 has a  $\beta$ -orientation.<sup>16,10,17</sup> The structure of compound **1** was confirmed by X-ray crystallography, which also allowed the absolute configuration to be assigned (Figure 2).<sup>18</sup> Thus, compound **1** was assigned as (1*S*,4*S*,5*S*,6*R*,7*R*,9*S*,10*S*)-1,6,11-triacetoxy-4-hydroxy-9-cinnamoyloxydihydro- $\beta$ -agarofuran and was assigned the trivial name denhaminol A (**1**).

Compound **2**, named denhaminol B, gave the elemental formula C<sub>30</sub>H<sub>38</sub>O<sub>11</sub>, which was assigned following analysis of the (+)-HRESIMS ion at  $m/z$  597.2314 [ $M + \text{Na}$ ]<sup>+</sup> (calcd 597.2306). The MS and NMR data revealed that compound **2** displayed a high degree of homology with denhaminol A (**1**). The <sup>1</sup>H NMR spectrum of **2** showed an additional downfield methine signal ( $\delta_{\text{H}}$  4.57) and only three sets of methylene protons ( $\delta_{\text{H}}$  1.43–1.97, 1.74–1.93, and 4.41–4.62) when

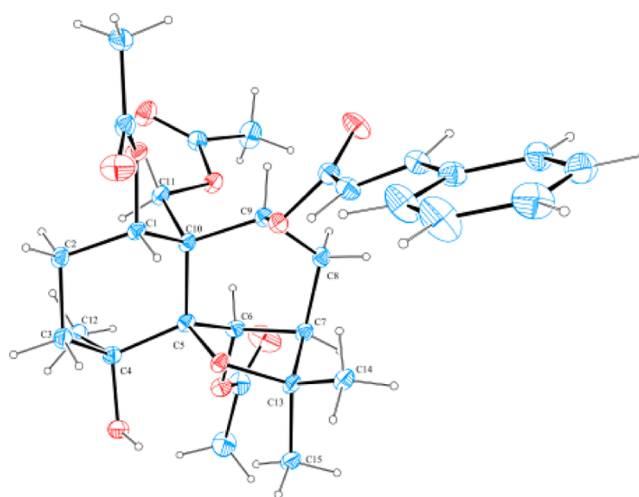


**Figure 2.** ORTEP of denhaminol A (**1**) (acetone solvate).

compared to **1**. The HSQC data showed the additional downfield methine signal ( $\delta_{\text{H}}$  4.57) was attached to an oxygenated carbon ( $\delta_{\text{C}}$  71.7). Furthermore, this additional proton was part of the spin system that constituted H-7/H-8/H-9 (Figure 3). The HMBC data in addition to the MS data

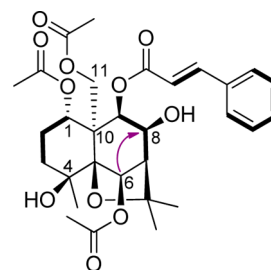


**Figure 3.** Selected HMBC ( $\rightarrow$ ) and COSY (bold line) correlations of denhaminol B (**2**).

indicated that the methylene proton (H-8) in **1** was replaced by a hydroxy methine group in **2**. The NOESY data were similar to those of **1**, with the exception of NOE correlations between the oxymethine proton H-8 and H-6, H-7, and H-9, which confirmed the  $\alpha$ -orientation of H-8. Thus, compound **2** was assigned as 1 *$\alpha$* ,6 *$\beta$* ,11-triacetoxy-4 *$\beta$* ,8 *$\beta$* -dihydroxy-9 *$\beta$* -cinnamoyloxydihydro- $\beta$ -agarofuran.

The molecular formula of denhaminol C (**3**) was determined to be C<sub>28</sub>H<sub>36</sub>O<sub>9</sub> according to the NMR and (+)-HRESIMS data. Analysis of the 1D and 2D NMR spectra of **3** indicated it was also structurally related to denhaminol A (**1**), the difference being the presence of two acetates ( $\delta_{\text{H}}$  1.81 and 2.18) and an additional hydroxy group ( $\delta_{\text{H}}$  5.12) in **3**, whereas denhaminol A displayed three *O*-acetyl singlets. This additional hydroxy group displayed HMBC correlations (Figure 4) to C-6 ( $\delta_{\text{H}}$  78.8) and C-5 ( $\delta_{\text{H}}$  91.1). Furthermore, H-6 resonated as a doublet in **3** with the same coupling constant ( $J = 5.3$  Hz) as the hydroxy group ( $\delta_{\text{H}}$  5.12). It was deduced that the *O*-acetyl group at C-6 in denhaminol A (**1**) was replaced in compound **3** by a hydroxy group. The NOE cross-peaks between the signal of H-7 and H-6 and as well as between H-9 and the methylene protons H-11 were used to determine the  $\alpha$ -orientation of both H-6 and H-9. Thus, compound **3** was assigned as 1 *$\alpha$* ,11-diacetoxy-4 *$\beta$* ,6 *$\beta$* -dihydroxy-9 *$\beta$* -cinnamoyloxydihydro- $\beta$ -agarofuran.

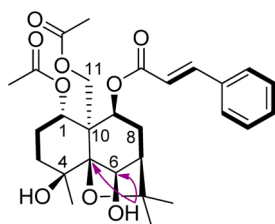


**Figure 4.** Selected HMBC ( $\rightarrow$ ) and COSY (bold line) correlations of denhaminol C (3).

Denhaminol D (4) was isolated as a stable white gum, with a molecular formula of  $C_{35}H_{40}O_{11}$ , which was established following analysis of the (+)-HRESIMS and NMR data. The  $^1H$  NMR spectrum of compound 4 showed only minor differences compared to denhaminol C (3). Denhaminol D (4) contained resonances for an extra benzoyl group ( $\delta_H$  7.99, 7.57, 7.44) and an additional set of methylene protons [ $\delta_H$  4.73, d ( $J$  = 11 Hz); 4.93, d ( $J$  = 11 Hz)], but was lacking a methyl group compared to 3. The HMBC data (Figure 5) for 4 showed

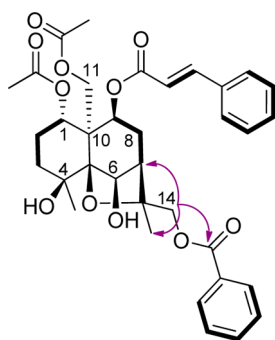


**Figure 5.** Selected HMBC ( $\rightarrow$ ) and COSY (bold line) correlations of denhaminol D (4).

correlations between the extra set of methylene protons and the benzoyl carbonyl ( $\delta_C$  166.1), C-7 ( $\delta_C$  49.0), and  $CH_3$ -15 ( $\delta_C$  25.2). These data suggested that the benzoyl group was attached to the dihydro- $\beta$ -agarofuran scaffold at C-14. The NOESY data for H-1, H-6, H-7, H-9, and H-11 were similar to those of denhaminol C (3), indicating the  $\beta$ -orientation of H-1 and the  $\alpha$ -orientation of H-6 and H-9. Thus, compound 4 was assigned as 1 $\alpha$ ,11-diacetoxy-4 $\beta$ ,6 $\beta$ -dihydroxy-9 $\beta$ -cinnamoyloxy-14-benzoyloxydihydro- $\beta$ -agarofuran.

Compound 5, named denhaminol E, was found to possess a molecular formula of  $C_{37}H_{42}O_{12}$ , following the interpretation of (+)-HRESIMS and NMR data. When comparing the  $^1H$  NMR spectra of 4 and 5, an additional *O*-acetyl signal in 5 ( $\delta_H$  2.13) suggested that OH-6 in 4 was acetylated in 5. This was confirmed by an HMBC correlation (Figure 6) between the methine proton H-6 ( $\delta_H$  6.16) and the *O*-acetyl carbonyl ( $\delta_C$  170.4) and by the fact that H-6 resonated as a singlet. The H-9 signal showed a NOE correlation to the methylene protons H-11, confirming the  $\alpha$ -orientation of the latter. The NOESY data also confirmed the  $\alpha$ -orientation of H-6 (NOE cross-peak with  $CH_3$ -12, H-7, and H-11). Thus, compound 5 was assigned as 1 $\alpha$ ,6 $\beta$ ,11-triacetoxy-4 $\beta$ -hydroxy-9 $\beta$ -cinnamoyloxy-14-benzoyloxydihydro- $\beta$ -agarofuran.

The molecular formula ( $C_{37}H_{42}O_{13}$ ) of 6 was established following interpretation of the  $^1H$  and  $^{13}C$  NMR data and the (+)-HRESIMS ion  $[M + Na]^+$  at  $m/z$  717.2512 (calcd 717.2518). Several small differences were apparent in the  $^1H$

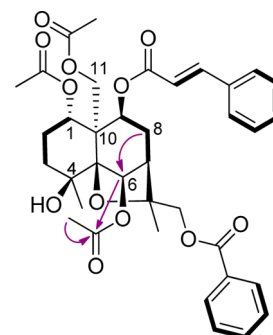


**Figure 6.** Selected HMBC ( $\rightarrow$ ) and COSY (bold line) correlations of denhaminol E (5).

NMR spectra of 5 and 6. For instance, two *O*-acetyl signals ( $\delta_H$  1.93 and 2.17) in 6 instead of three signals in 5 were observed, as well as four sets of methylene protons ( $\delta_H$  4.35–4.47, 4.93, 1.50–1.93, 1.71–1.88) in 6, whereas 5 exhibited signals for five sets of methylene protons. Furthermore, the  $^1H$  NMR spectrum of 6 displayed an additional methyl group ( $\delta_H$  1.38) and an extra methine proton ( $\delta_H$  4.55). The lack of one methylene in 6 compared to denhaminol E (5), in conjunction with the extra methine proton ( $\delta_H$  4.55, dd,  $J$  = 6.4, 3.2 Hz) in 6, and the COSY (H-7/H-8/H-9) and HMBC (H-6/C-8) correlations (Figure 7), indicated a hydroxy group at C-

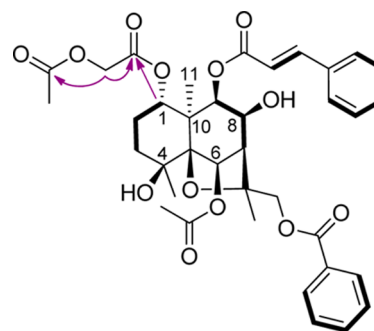


**Figure 7.** Selected HMBC ( $\rightarrow$ ) and COSY (bold line) correlations of denhaminol F (6).

8. The H-1 ( $\delta_H$  5.40) and H-9 ( $\delta_H$  5.13) signals exhibited HMBC correlations to the extra methyl group resonance ( $\delta_C$  19.6). Moreover, this same methyl group showed a strong HMBC correlation to the quaternary carbon at  $\delta_C$  49.9, confirming the presence of a methyl at C-10 in 6. The set of methylene protons at  $\delta_H$  4.35 and 4.47 showed HMBC correlations to the carbonyl carbons resonating at  $\delta_C$  170.0 and 167.6. These data along with the HMBC correlations between the methine proton H-1 ( $\delta_H$  5.40) and the carbonyl at  $\delta_C$  167.6 as well as from the methyl at  $\delta_H$  1.93 to the carbonyl carbon at  $\delta_C$  170.0 suggested that the substituent at C-1 was an acetoxyacetate.<sup>19</sup> The relative configuration of 6 was assigned following NOESY data analysis. NOESY correlations between H-6 and H-7 and  $CH_3$ -11 and  $CH_3$ -12, as well as cross-peaks between H-8 and H-7 and  $CH_3$ -11 and NOEs observed from H-9 and  $CH_3$ -11, confirmed the  $\alpha$ -orientation of H-6, H-8, and H-9. Thus, compound 6 was assigned as 1 $\alpha$ -acetoxyacetate-4 $\beta$ ,8 $\beta$ -dihydroxy-6 $\beta$ -acetoxy-9 $\beta$ -cinnamoyloxy-14-benzoyloxydihydro- $\beta$ -agarofuran and was given the trivial name denhaminol F (6). This is only the second report of a dihydro- $\beta$ -agarofuran containing an acetoxyacetate functional



group, with the first one being vaalens-3, which was isolated in 1990 by Begley et al.<sup>20</sup>

The minor metabolite, compound 7, was assigned the molecular formula  $C_{35}H_{44}O_{13}$  following (+)-HRESIMS and NMR data analysis. These data indicated that, in comparison to denhaminol F (6), compound 7 did not contain a benzoyl group. However, additional signals that corresponded to one olefinic methine proton ( $\delta_H$  6.86) and two deshielded methyl groups ( $\delta_H$  1.80 and 1.81) were present in the  $^1H$  NMR spectrum of 7. COSY data (Figure 8) and the multiplicity and

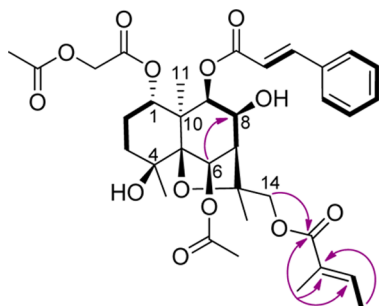


**Figure 8.** Selected HMBC ( $\rightarrow$ ) and COSY (bold line) correlations of denhaminol G (7).

coupling constant of the olefinic methine at  $\delta_H$  6.86 (q,  $J$  = 6.6 Hz) indicated this proton to be geminal to one methyl group ( $\delta_H$  1.80, d,  $J$  = 6.6 Hz). The HMBC data between the second deshielded methyl ( $\delta_H$  1.81), the carbonyl ( $\delta_C$  167.9), and the carbon bearing both the olefinic methine proton and the vicinal methyl were used to establish a 2-methyl-2-butenic acid moiety.<sup>21</sup> The chemical shifts and coupling constants were typical of a tiglic acid moiety.<sup>21</sup> This *E* configuration was confirmed by comparison of  $^1H$  NMR data with commercially available tiglic and angelic acids (Figures S42–S45, Supporting Information). The set of methylene protons at C-14 ( $\delta_H$  4.71–4.76) displayed HMBC correlations to the tiglic carbonyl ( $\delta_C$  167.9), confirming that the benzoyl group in 6 was replaced by a tigloyl group in 7. The NOESY spectra of 6 and 7 were identical in relation to H-6, H-8, and H-9, indicating the  $\alpha$ -orientation of these methine protons. Thus, compound 7 was assigned as 1 $\alpha$ -acetoxyacetate-4 $\beta$ ,8 $\beta$ -dihydroxy-6 $\beta$ -acetoxy-9 $\beta$ -cinnamoyloxy-14-tigloyloxydihydro- $\beta$ -agarofuran and was given the trivial name denhaminol G (7).

The final dihydro- $\beta$ -agarofuran of the series, denhaminol H (8), was assigned a molecular formula of  $C_{37}H_{46}O_{14}$ , following (+)-HRESIMS and NMR data analysis. The 1D and 2D NMR data of compound 8 closely resembled those of denhaminol G (7); however data comparison showed that 8 contained an extra *O*-acetyl signal ( $\delta_H$  2.25,  $\delta_C$  21.2) and two additional sets of methylene protons ( $\delta_H$  4.41–4.62 and 2.18–2.51) and lacked a methyl signal that was present in 7. These observations indicated that 8 possessed an *O*-acetyl group at C-11, which was confirmed by HMBC correlations (Figure 9) from the methylene protons ( $\delta_H$  4.41 and 4.62) to the quaternary carbon C-10 ( $\delta_C$  54.0) and to the acetyl carbonyl at  $\delta_C$  170.4. Chemical shift and COSY and HMBC correlations were used to position the remaining methylene protons ( $\delta_H$  2.18 and 2.51) at C-8. NOE cross-peaks between the signal of H-11 and H-6 and H-9 were used to determine their  $\alpha$ -orientation. Thus, compound 8 was assigned as 1 $\alpha$ -acetoxyacetate-4 $\beta$ -hydroxy-6 $\beta$ ,11-diacetoxy-9 $\beta$ -cinnamoyloxy-14-tigloyloxydihydro- $\beta$ -agarofuran.

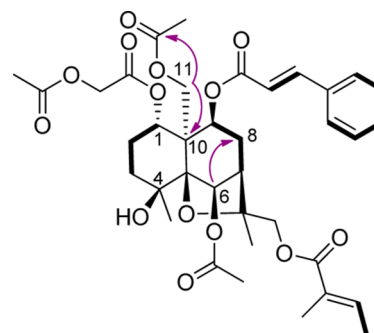


**Figure 9.** Selected HMBC ( $\rightarrow$ ) and COSY (bold line) correlations of denhaminol H (8).

Due to our interest in the discovery of new small molecules that inhibit the growth of prostate cancer cells,<sup>22,23</sup> denhaminols A–H (1–8) were tested against the LNCaP cell line (human prostate carcinoma), using a metabolic assay (AlamarBlue). All compounds were found to have an  $IC_{50}$  greater than 10  $\mu$ M after 72 h of treatment (Figure S46, Supporting Information). The effect of denhaminols A–H (1–8) on cell growth was also evaluated using a live-cell imaging based assay. Proliferation of LNCaP cells was monitored as a function of cell confluence, using an IncuCyte system (Figures S47 and S48, Supporting Information). Denhaminol G (7) showed the most significant biological response in this assay. During the first hours of treatment with 7, cell confluence and morphology were similar to the DMSO control (Figures 10A). However, in a time- and concentration-dependent manner, cells became flat, enlarged, and highly granular and eventually burst (Figure 10B). The growth profile and cell morphology of LNCaP cells treated with 7 showed similarities to those described by Sadowski et al.,<sup>24</sup> where LNCaP cells were treated with the acetyl-CoA carboxylase inhibitor TOFA or the fatty acid synthase inhibitor orlistat,<sup>25</sup> which both inhibit de novo synthesis of fatty acids.<sup>26,27</sup> To further investigate the possibility that the denhaminol-induced morphological phenotype was caused by changes to the cellular lipid levels, LNCaP cells were treated with the two major natural products denhaminols A (1, 60  $\mu$ M) and G (7, 25  $\mu$ M), TOFA (10  $\mu$ M), and DMSO (negative control), and the cellular lipid content was analyzed by fluorescence microscopy. As shown in Figure 11A, denhaminol A (1) and TOFA visibly reduced the neutral lipid (sterols, triglycerides, and fatty acids, which are mainly found in lipid droplets) content when compared to control (DMSO). Quantitative analysis demonstrated that denhaminols A (1) and G (7) significantly reduced the cellular levels of both neutral lipids and phospholipids (phosphatidylcholine, phosphatidylethanolamine, and phosphatidylserine, which are major components of cell membranes), in a similar fashion as TOFA (Figure 11B and C).

One of the striking hallmarks of cancer is the reprogramming of metabolic pathways such as lipid synthesis (reviewed by Zhang et al.<sup>28</sup>). Despite the abundance of exogenous fatty acids provided through the diet, cancer cells synthesize most of their required saturated and monounsaturated fatty acids de novo through enhanced lipogenesis. Dysregulation of lipogenesis has been found in almost all types of cancer and is critical during the early process of transformation, cancer cell survival, and tumorigenesis and is associated with the aggressiveness of the disease. This unique requirement for de novo lipid synthesis provides an excellent target for pharmacological intervention.<sup>28</sup>

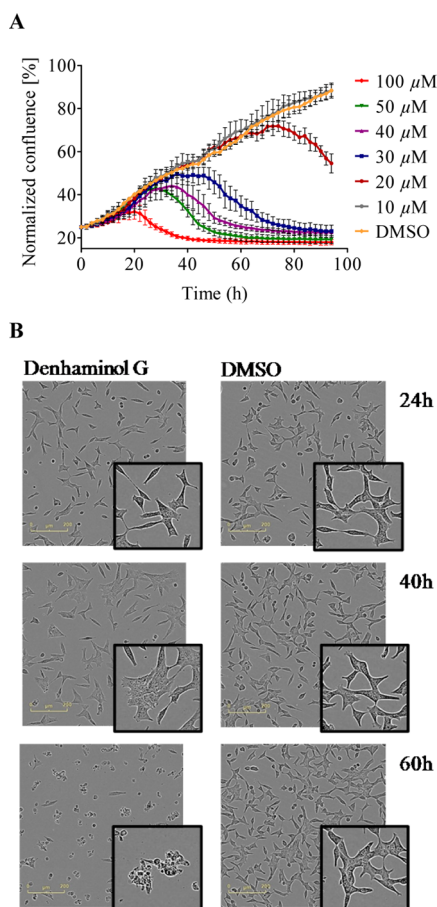


**Figure 10.** (A) Changes to cell confluence and (B) cell morphology of LNCaP cells after treatment with indicated concentrations of denhaminol G (7, 40  $\mu$ M) monitored with an IncuCyte real-time live-cell imaging system (scale bar: 200  $\mu$ m).

The discovery that denhaminols A and G affect lipid homeostasis and reduce the lipid content of LNCaP prostate cancer cells warrants further investigation.

## EXPERIMENTAL SECTION

**General Experimental Procedures.** Melting points were determined using a Cole-Parmer (Vernon Hills, IL, USA) melting point apparatus and were uncorrected. Optical rotations were recorded on a JASCO P-1020 polarimeter (Easton, MD, USA). IR and UV spectra were recorded on a Bruker Tensor 27 spectrophotometer (Billerica, MA, USA) and a JASCO V-650 UV/vis spectrophotometer, respectively. NMR spectra were recorded at 30  $^{\circ}$ C on a Varian 600 MHz Unity INOVA spectrometer (Palo Alto, CA, USA). The  $^1$ H and  $^{13}$ C chemical shifts were referenced to the solvent peaks for  $\text{CDCl}_3$  at  $\delta_{\text{H}}$  7.27 and  $\delta_{\text{C}}$  77.0, respectively. Standard parameters were used for the 2D NMR experiments, which included HSQC ( $^1J_{\text{CH}}$  = 140 Hz) and HMBC ( $^nJ_{\text{CH}}$  = 4.0 Hz). LRESIMS data were recorded on a Waters LC-MS system (Milford, MA, USA) equipped with a Phenomenex Luna C<sub>18</sub> column (3  $\mu$ m, 100 Å, 4.6  $\times$  50 mm, Torrance, CA, USA), a PDA detector, and a ZQ ESI mass spectrometer. HRESIMS were recorded on a Bruker MicrOTof-Q spectrometer (Dionex UltiMate 3000 micro LC system, ESI mode). All solvents used for chromatography,  $[\alpha]_{\text{D}}$ , UV, and MS were Lab-Scan HPLC grade (Gliwice, Poland), and the  $\text{H}_2\text{O}$  was Millipore Milli-Q PF filtered (Billerica, MA, USA). Merck silica gel 60 (0.04–0.063 mm, Billerica, MA, USA) packed into an open glass column (23  $\times$  5 cm) was used for flash chromatography. Thin-layer chromatography (TLC) was performed on Merck silica gel 60 F254 precoated aluminum plates and was observed using UV light. Phenomenex end-

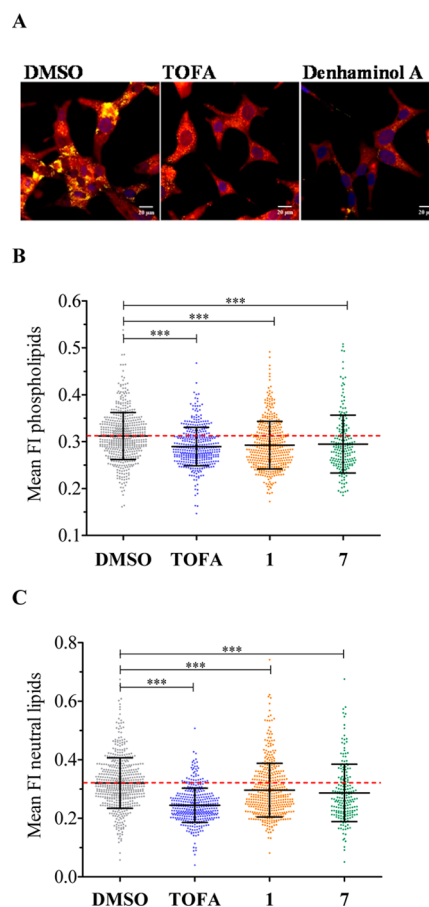


**Figure 11.** (A) LNCaP cells treated with 60  $\mu$ M of denhaminol A (1), 10  $\mu$ M of TOFA, or DMSO as vehicle control for 72 h. Neutral lipids (yellow) and phospholipids (red) were stained with Nile Red, DNA, with DAPI (blue), and cells were visualized by fluorescence microscopy on a Cytell cell imaging system (scale bar: 20  $\mu$ m). (B) Phospholipid and (C) neutral lipid content of LNCaP cells treated for 72 h with 10  $\mu$ M TOFA (positive control), denhaminol A (1, 60  $\mu$ M), and denhaminol G (7, 25  $\mu$ M). The mean fluorescence intensities (FI) of cellular neutral lipids and phospholipids of Nile Red-stained LNCaP cells were quantified with CellProfiler ( $n \sim 300$  cells, mean  $\pm$  SD, one-way ANOVA with Dunnett's multiple comparison test, \*\*\* $p$  < 0.001).

capped Septra C<sub>18</sub> bonded silica (35–75  $\mu$ m, 150 Å) was used for fraction preadsorption work, and the resulting material was packed into an Alltech stainless steel guard cartridge (10  $\times$  30 mm, Columbia, MD, USA). A Waters pump 600 fitted with a Waters 996 photodiode array detector and Gilson 717 plus autosampler (Middleton, WI, USA) was used for semipreparative and analytical HPLC separations. A Thermo Fisher Scientific Betasil phenyl column (5  $\mu$ m, 143 Å, 21.2  $\times$  150 mm, Waltham, MA, USA) was used for semipreparative HPLC. A Fritsch Universal Cutting Mill Pulverisette 19 (Idar-Oberstein, Germany) was used to grind the air-dried plant material. An Edwards Instrument Company Bioline orbital shaker (Narangba, Australia) was used for the large-scale plant extractions. Tiglic acid and angelic acid were purchased from Sigma-Aldrich (St. Louis, MO, USA) and ACBR (Karlsruhe, Germany), respectively.

**Plant Material.** Leaves of *Denhamia celastroides* (F. Muell.) Jessup (Celastraceae) were collected from Walton Bridge Reserve, The Gap, Australia, in October 2012. A voucher specimen (RAD059) has been deposited at the Eskitis Institute for Drug Discovery, Griffith University, Brisbane, Australia. The plant material was air-dried, ground to a fine powder, and stored at room temperature prior to extraction.

**Extraction and Isolation.** The air-dried and ground leaves of *D. celastroides* (55 g) were poured into a conical flask (1 L),  $\text{CH}_2\text{Cl}_2$  (500

mL) was added, and the mixture was shaken on the orbital shaker at 200 rpm for 2 h at room temperature. The resulting extract was filtered under gravity and set aside. This extraction process was repeated three times to yield a  $\text{CH}_2\text{Cl}_2$  extract (2500 mL), which was dried under reduced pressure to yield a dark green gum (2.0 g). A portion of the  $\text{CH}_2\text{Cl}_2$  extract (1.6 g) was resuspended in MeOH and subjected to silica flash chromatography using a stepwise gradient elution from 80% *n*-hexane/20% EtOAc to 100% EtOAc. One-hundred fractions (100 × 20 mL) were collected and analyzed by TLC. The fractions containing dihydro- $\beta$ -agarofurans were further investigated by LC-MS and  $^1\text{H}$  NMR spectroscopy. Fractions 56–62 (60 mg) were combined, dried down, preadsorbed to  $\text{C}_{18}$  bonded silica, and packed into a stainless steel cartridge. This cartridge was subsequently attached to a semipreparative Betasil phenyl HPLC column, and linear gradient conditions from 50% MeOH (0.1% TFA)/50%  $\text{H}_2\text{O}$  (0.1% TFA) to 90% MeOH (0.1% TFA)/10%  $\text{H}_2\text{O}$  (0.1% TFA) were run over 50 min at a flow rate of 9 mL/min. Fifteen fractions (15 × 1 min) were collected between 33 and 48 min, and two pure compounds were obtained, denhaminol C (**3**,  $t_R$  = 34–35 min, 5.0 mg, 0.008% dry wt) and denhaminol A (**1**,  $t_R$  = 40 min, 7.0 mg, 0.011% dry wt). Fractions 71–73 (16 mg) obtained from the first isolation step were combined and further purified by HPLC using a phenyl column with solvent conditions consisting of a linear gradient from 65% MeOH (0.1% TFA)/35%  $\text{H}_2\text{O}$  (0.1% TFA) to 90% MeOH (0.1% TFA)/10%  $\text{H}_2\text{O}$  (0.1% TFA) in 50 min at a flow rate of 9 mL/min. Thirty-five fractions (35 × 1 min) were collected between 16 and 51 min, and two pure compounds were obtained, denhaminol D (**4**,  $t_R$  = 32 min, 1.2 mg, 0.002% dry wt) and denhaminol E (**5**,  $t_R$  = 37 min, 2.4 mg, 0.004% dry wt). Fractions 75–77 (16 mg) obtained from the first isolation step were combined and further purified by HPLC using a Betasil phenyl column with solvent conditions consisting of a linear gradient from 65% MeOH (0.1% TFA)/35%  $\text{H}_2\text{O}$  (0.1% TFA) to 90% MeOH (0.1% TFA)/10%  $\text{H}_2\text{O}$  (0.1% TFA) in 50 min at a flow rate of 9 mL/min. Thirty-four fractions (34 × 1 min) were collected between 16 and 51 min, and two pure compounds were obtained, denhaminol B (**2**,  $t_R$  = 17–18 min, 3.1 mg, 0.005% dry wt) and denhaminol H (**7**,  $t_R$  = 33 min, 1.0 mg, 0.002% dry wt). Fractions 83–90 (m = 12 mg) obtained from the first isolation step were combined and further purified by HPLC using a phenyl column with solvent conditions consisting of a linear gradient from 50% MeOH (0.1% TFA)/50%  $\text{H}_2\text{O}$  (0.1% TFA) to 90% MeOH (0.1% TFA)/10%  $\text{H}_2\text{O}$  (0.1% TFA) performed over 50 min at a flow rate of 9 mL/min. Twenty-nine fractions (29 × 1 min) were collected between 21 and 50 min, and two pure compounds were obtained, denhaminol G (**8**,  $t_R$  = 37 min, 7.3 mg, 0.011% dry wt) and denhaminol F (**6**,  $t_R$  = 39 min, 1.2 mg, 0.002% dry wt).

**Denhaminol A (1):** colorless needles (acetone); mp 161–163 °C;  $[\alpha]_D^{25} +25.6$  (c 0.1, MeOH); UV (MeOH)  $\lambda_{\text{max}}$  (log  $\epsilon$ ) 280 (3.86), 223 (3.67), 217 (3.86) nm; IR (KBr)  $\nu_{\text{max}}$  3544, 2933, 2855, 1739, 1713, 1636, 1368, 1239, 1029, 875, 713  $\text{cm}^{-1}$ ;  $^1\text{H}$  NMR ( $\text{CDCl}_3$ , 600 MHz) see Table 1 and  $\delta_{\text{H}}$  7.69 (1H, d,  $J$  = 15.9 Hz, *trans*-OCin-9), 7.54 (2H, m, *trans*-OCin-9), 7.41 (1H, m, *trans*-OCin-9), 7.40 (2H, m, *trans*-OCin-9), 6.37 (1H, d,  $J$  = 15.9 Hz, *trans*-OCin-9), 2.25 (3H, s, OAc-11), 2.10 (3H, s, OAc-6), 1.81 (3H, s, OAc-1);  $^{13}\text{C}$  NMR ( $\text{CDCl}_3$ , 150 MHz) see Table 3 and  $\delta_{\text{C}}$  170.4 (C, OAc-11), 170.2 (C, OAc-6), 169.9 (C, OAc-1), 165.5 (C, *trans*-OCin-9), 145.6 (CH, *trans*-OCin-9), 134.2 (C, *trans*-OCin-9), 130.8 (CH, *trans*-OCin-9), 128.9 (CH, *trans*-OCin-9), 128.2 (CH, *trans*-OCin-9), 117.4 (CH, *trans*-OCin-9), 21.5 (CH<sub>3</sub>, OAc-6), 21.1 (CH<sub>3</sub>, OAc-11), 21.0 (CH<sub>3</sub>, OAc-1); (+)-LRESIMS  $m/z$  541 (100)  $[\text{M} - \text{OH}]^+$ , 581 (60)  $[\text{M} + \text{Na}]^+$ ; (+)-HRESIMS  $m/z$  581.2361  $[\text{M} + \text{Na}]^+$  (calcd for  $\text{C}_{30}\text{H}_{38}\text{O}_{10}\text{Na}$ , 581.2357).

**Denhaminol B (2):** stable white gum;  $[\alpha]_D^{25} +81.0$  (c 0.03, MeOH); UV (MeOH)  $\lambda_{\text{max}}$  (log  $\epsilon$ ) 279 (4.02), 222 (3.78), 217 (3.84) nm; IR (KBr)  $\nu_{\text{max}}$  3501, 3029, 2855, 1741, 1636, 1496, 1369, 1231, 1163, 1054, 736  $\text{cm}^{-1}$ ;  $^1\text{H}$  NMR ( $\text{CDCl}_3$ , 600 MHz) see Table 1 and  $\delta_{\text{H}}$  7.75 (1H, d,  $J$  = 15.9 Hz, *trans*-OCin-9), 7.58 (2H, m, *trans*-OCin-9), 7.43 (1H, m, *trans*-OCin-9), 7.42 (2H, m, *trans*-OCin-9), 6.45 (1H, d,  $J$  = 15.9 Hz, *trans*-OCin-9), 2.25 (3H, s, OAc-11), 2.11 (3H, s, OAc-6), 1.83 (3H, s, OAc-1);  $^{13}\text{C}$  NMR ( $\text{CDCl}_3$ , 150 MHz) see Table 3 and  $\delta_{\text{C}}$  170.4 (C, OAc-11), 170.1 (C, OAc-6), 169.5 (C, OAc-1), 167.6

(C, *trans*-OCin-9), 146.7 (CH, *trans*-OCin-9), 134.2 (C, *trans*-OCin-9), 130.8 (CH, *trans*-OCin-9), 128.7 (CH, *trans*-OCin-9), 128.4 (CH, *trans*-OCin-9), 117.2 (CH, *trans*-OCin-9), 21.6 (CH<sub>3</sub>, OAc-6), 21.3 (CH<sub>3</sub>, OAc-11), 21.0 (CH<sub>3</sub>, OAc-1); (+)-LRESIMS  $m/z$  557 (100)  $[\text{M} - \text{OH}]^+$ , 575 (80)  $[\text{M} + \text{H}]^+$ , 597 (30)  $[\text{M} + \text{Na}]^+$ ; (+)-HRESIMS  $m/z$  597.2314  $[\text{M} + \text{Na}]^+$  (calcd for  $\text{C}_{30}\text{H}_{38}\text{O}_{11}\text{Na}$ , 597.2306).

**Denhaminol C (3):** stable white gum;  $[\alpha]_D^{25} +63.0$  (c 0.03, MeOH); UV (MeOH)  $\lambda_{\text{max}}$  (log  $\epsilon$ ) 280 (4.03), 223 (3.81), 217 (3.86) nm; IR (KBr)  $\nu_{\text{max}}$  3566, 3029, 2854, 1741, 1636, 1496, 1367, 1233, 1158, 1050, 737  $\text{cm}^{-1}$ ;  $^1\text{H}$  NMR ( $\text{CDCl}_3$ , 600 MHz) see Table 1 and  $\delta_{\text{H}}$  7.69 (1H, d,  $J$  = 15.9 Hz, *trans*-OCin-9), 7.55 (2H, m, *trans*-OCin-9), 7.40 (1H, m, *trans*-OCin-9), 7.39 (2H, m, *trans*-OCin-9), 6.35 (1H, d,  $J$  = 15.9 Hz, *trans*-OCin-9), 2.18 (3H, s, OAc-11), 1.81 (3H, s, OAc-1);  $^{13}\text{C}$  NMR ( $\text{CDCl}_3$ , 150 MHz) see Table 3 and  $\delta_{\text{C}}$  170.4 (C, OAc-11), 169.8 (C, OAc-1), 165.6 (C, *trans*-OCin-9), 145.8 (CH, *trans*-OCin-9), 134.2 (C, *trans*-OCin-9), 130.4 (CH, *trans*-OCin-9), 128.9 (CH, *trans*-OCin-9), 128.2 (CH, *trans*-OCin-9), 117.5 (CH, *trans*-OCin-9), 21.4 (CH<sub>3</sub>, OAc-11), 21.0 (CH<sub>3</sub>, OAc-1); (+)-LRESIMS  $m/z$  499 (100)  $[\text{M} - \text{OH}]^+$ , 517 (20)  $[\text{M} + \text{H}]^+$ , 539 (50)  $[\text{M} + \text{Na}]^+$ ; (+)-HRESIMS  $m/z$  539.2250  $[\text{M} + \text{Na}]^+$  (calcd for  $\text{C}_{28}\text{H}_{36}\text{O}_9\text{Na}$ , 539.2252).

**Denhaminol D (4):** stable white gum;  $[\alpha]_D^{25} +27.0$  (c 0.03, MeOH); UV (MeOH)  $\lambda_{\text{max}}$  (log  $\epsilon$ ) 280 (3.94), 224 (4.06), 218 (4.05) nm; IR (KBr)  $\nu_{\text{max}}$  3503, 3031, 2854, 1742, 1718, 1637, 1489, 1367, 1232, 1155, 1049, 769, 713  $\text{cm}^{-1}$ ;  $^1\text{H}$  NMR ( $\text{CDCl}_3$ , 600 MHz) see Table 1 and  $\delta_{\text{H}}$  7.99 (2H, d,  $J$  = 7.7 Hz, OBz-14), 7.68 (1H, d,  $J$  = 15.9 Hz, *trans*-OCin-9), 7.57 (1H, t,  $J$  = 7.6 Hz, OBz-14), 7.55 (2H, br d,  $J$  = 7.8 Hz, *trans*-OCin-9), 7.44 (2H, dd,  $J$  = 7.7, 7.6 Hz, OBz-14), 7.36 (1H, m, *trans*-OCin-9), 7.35 (2H, m, *trans*-OCin-9), 6.45 (1H, d,  $J$  = 15.9 Hz, *trans*-OCin-9), 2.19 (3H, s, OAc-11), 1.81 (3H, s, OAc-1);  $^{13}\text{C}$  NMR ( $\text{CDCl}_3$ , 150 MHz) see Table 3 and  $\delta_{\text{C}}$  170.6 (C, OAc-11), 169.5 (C, OAc-1), 166.1 (C, OBz-14), 165.5 (C, *trans*-OCin-9), 146.4 (CH, *trans*-OCin-9), 134.3 (C, *trans*-OCin-9), 133.2 (CH, OBz-14), 131.0 (C, OBz-14), 130.5 (CH, *trans*-OCin-9), 129.5 (CH, OBz-14), 128.6 (CH, *trans*-OCin-9), 128.4 (CH, OBz-14), 128.2 (CH, *trans*-OCin-9), 117.4 (CH, *trans*-OCin-9), 21.4 (CH<sub>3</sub>, OAc-11), 20.9 (CH<sub>3</sub>, OAc-1); (+)-LRESIMS  $m/z$  619 (40)  $[\text{M} - \text{OH}]^+$ , 637 (60)  $[\text{M} + \text{H}]^+$ , 659 (100)  $[\text{M} + \text{Na}]^+$ ; (+)-HRESIMS  $m/z$  659.2458  $[\text{M} + \text{Na}]^+$  (calcd for  $\text{C}_{35}\text{H}_{40}\text{O}_{11}\text{Na}$ , 659.2463).

**Denhaminol E (5):** stable white gum;  $[\alpha]_D^{25} -9.6$  (c 0.07, MeOH); UV (MeOH)  $\lambda_{\text{max}}$  (log  $\epsilon$ ) 280 (4.13), 224 (4.21), 219 (4.19) nm; IR (KBr)  $\nu_{\text{max}}$  3566, 3030, 2856, 1741, 1718, 1636, 1490, 1369, 1236, 1159, 1050, 769, 713  $\text{cm}^{-1}$ ;  $^1\text{H}$  NMR ( $\text{CDCl}_3$ , 600 MHz) see Table 2 and  $\delta_{\text{H}}$  7.98 (2H, d,  $J$  = 7.6 Hz, OBz-14), 7.70 (1H, d,  $J$  = 15.9 Hz, *trans*-OCin-9), 7.57 (1H, t,  $J$  = 7.4 Hz, OBz-14), 7.55 (2H, br d,  $J$  = 7.8 Hz, *trans*-OCin-9), 7.43 (2H, dd,  $J$  = 7.6, 7.4 Hz, OBz-14), 7.37 (1H, m, *trans*-OCin-9), 7.36 (2H, m, *trans*-OCin-9), 6.45 (1H, d,  $J$  = 15.9 Hz, *trans*-OCin-9), 2.26 (3H, s, OAc-11), 2.13 (3H, s, OAc-6), 1.82 (3H, s, OAc-1);  $^{13}\text{C}$  NMR ( $\text{CDCl}_3$ , 150 MHz) see Table 3 and  $\delta_{\text{C}}$  170.4 (C, OAc-6), 170.2 (C, OAc-11), 169.9 (C, OAc-1), 166.1 (C, OBz-14), 165.4 (C, *trans*-OCin-9), 146.6 (CH, *trans*-OCin-9), 134.3 (C, *trans*-OCin-9), 133.1 (CH, OBz-14), 131.0 (C, OBz-14), 130.4 (CH, *trans*-OCin-9), 129.6 (CH, OBz-14), 128.8 (CH, *trans*-OCin-9), 128.5 (CH, *trans*-OCin-9), 128.4 (CH, OBz-14), 117.4 (CH, *trans*-OCin-9), 21.5 (CH<sub>3</sub>, OAc-6), 21.0 (CH<sub>3</sub>, OAc-11), 20.9 (CH<sub>3</sub>, OAc-1); (+)-LRESIMS  $m/z$  679 (100)  $[\text{M} + \text{H}]^+$ , 701 (50)  $[\text{M} + \text{Na}]^+$ ; (+)-HRESIMS  $m/z$  701.2564  $[\text{M} + \text{Na}]^+$  (calcd for  $\text{C}_{37}\text{H}_{42}\text{O}_{12}\text{Na}$ , 701.2568).

**Denhaminol F (6):** stable white gum;  $[\alpha]_D^{25} +45.0$  (c 0.03, MeOH); UV (MeOH)  $\lambda_{\text{max}}$  (log  $\epsilon$ ) 279 (3.91), 224 (4.01), 218 (3.98) nm; IR (KBr)  $\nu_{\text{max}}$  3502, 2925, 2854, 1742, 1717, 1637, 1451, 1374, 1231, 1163, 1054, 769, 714  $\text{cm}^{-1}$ ;  $^1\text{H}$  NMR ( $\text{CDCl}_3$ , 600 MHz) see Table 2 and  $\delta_{\text{H}}$  8.02 (2H, d,  $J$  = 7.8 Hz, OBz-14), 7.71 (1H, d,  $J$  = 15.9 Hz, *trans*-OCin-9), 7.57 (1H, t,  $J$  = 7.6 Hz, OBz-14), 7.54 (2H, br d,  $J$  = 7.3 Hz, *trans*-OCin-9), 7.45 (2H, dd,  $J$  = 7.8, 7.6 Hz, OBz-14), 7.35 (1H, m, *trans*-OCin-9), 7.34 (2H, m, *trans*-OCin-9), 6.51 (1H, d,  $J$  = 15.9 Hz, *trans*-OCin-9), 4.47 (1H, d,  $J$  = 15.8 Hz, OAcAc-1), 4.35 (1H, d,  $J$  = 15.8 Hz, OAcAc-1), 2.17 (3H, s, OAc-6), 1.93 (3H, s, OAcAc-1);  $^{13}\text{C}$  NMR ( $\text{CDCl}_3$ , 150 MHz) see Table 3 and  $\delta_{\text{C}}$  170.2 (C, OAc-6), 170.0 (C, OAcAc-1), 167.8 (C, *trans*-OCin-9), 167.6 (C, OAcAc-1),



166.1 (C, OBz-14), 146.9 (CH, *trans*-OCin-9), 134.7 (C, *trans*-OCin-9), 133.0 (CH, OBz-14), 131.0 (C, OBz-14), 130.2 (CH, *trans*-OCin-9), 129.1 (CH, OBz-14), 128.8 (CH, *trans*-OCin-9), 128.6 (CH, *trans*-OCin-9), 128.5 (CH, OBz-14), 117.0 (CH, *trans*-OCin-9), 60.6 (CH<sub>2</sub>, OAcAc-1), 21.4 (CH<sub>3</sub>, OAc-6), 20.4 (CH<sub>3</sub>, OAcAc-1); (+)-LRESIMS *m/z* 695 (100) [M + H]<sup>+</sup>, 717 (10) [M + Na]<sup>+</sup>; (+)-HRESIMS *m/z* 717.2512 [M + Na]<sup>+</sup> (calcd for C<sub>37</sub>H<sub>42</sub>O<sub>13</sub>Na, 717.2518).

**Denhaminol G (7):** stable white gum; [ $\alpha$ ]<sub>D</sub><sup>25</sup> +40.0 (c 0.02, MeOH); UV (MeOH)  $\lambda_{\max}$  (log  $\epsilon$ ) 280 (3.87), 223 (3.89), 218 (3.94) nm; IR (KBr)  $\nu_{\max}$  3051, 2929, 1747, 1714, 1637, 1374, 1269, 1054, 892, 703 cm<sup>-1</sup>; <sup>1</sup>H NMR (CDCl<sub>3</sub>, 600 MHz) see Table 2 and  $\delta_{\text{H}}$  7.70 (1H, d, *J* = 15.9 Hz, *trans*-OCin-9), 7.60 (2H, m, *trans*-OCin-9), 7.41 (1H, m, *trans*-OCin-9), 7.40 (2H, m, *trans*-OCin-9), 6.86 (1H, q, *J* = 6.6 Hz, OTig-14), 6.48 (1H, d, *J* = 15.9 Hz, *trans*-OCin-9), 4.47 (1H, d, *J* = 15.8 Hz, OAcAc-1), 4.36 (1H, d, *J* = 15.8 Hz, OAcAc-1), 2.15 (3H, s, OAc-6), 1.94 (3H, s, OAcAc-1), 1.81 (3H, s, OTig-14), 1.80 (3H, d, *J* = 6.6 Hz, OTig-14); <sup>13</sup>C NMR (CDCl<sub>3</sub>, 150 MHz) see Table 3 and  $\delta_{\text{C}}$  170.2 (C, OAc-6), 170.0 (C, OAcAc-1), 167.9 (C, *trans*-OCin-9), 167.6 (C, OTig-14), 166.8 (C, OAcAc-1), 146.7 (CH, *trans*-OCin-9), 137.0 (CH, OTig-14), 134.3 (C, *trans*-OCin-9), 130.5 (CH, *trans*-OCin-9), 128.7 (CH, *trans*-OCin-9), 128.5 (CH, *trans*-OCin-9), 128.0 (C, OTig-14), 117.4 (CH, *trans*-OCin-9), 60.7 (CH<sub>2</sub>, OAcAc-1), 21.5 (CH<sub>3</sub>, OAc-6), 20.5 (CH<sub>3</sub>, OAcAc-1), 14.2 (CH<sub>3</sub>, OTig-14), 12.0 (CH<sub>3</sub>, OTig-14); (+)-LRESIMS *m/z* 673 (100) [M + H]<sup>+</sup>, 695 (20) [M + Na]<sup>+</sup>; (+)-HRESIMS *m/z* 695.2680 [M + Na]<sup>+</sup> (calcd for C<sub>35</sub>H<sub>44</sub>O<sub>13</sub>Na, 695.2674).

**Denhaminol H (8):** stable white gum; [ $\alpha$ ]<sub>D</sub><sup>25</sup> +12.0 (c 0.03, MeOH); UV (MeOH)  $\lambda_{\max}$  (log  $\epsilon$ ) 281 (4.25), 223 (4.30) nm; IR (KBr)  $\nu_{\max}$  3567, 2925, 2854, 1748, 1716, 1375, 1238, 877, 770, 669 cm<sup>-1</sup>; <sup>1</sup>H NMR (CDCl<sub>3</sub>, 600 MHz) see Table 2 and  $\delta_{\text{H}}$  7.68 (1H, d, *J* = 15.9 Hz, *trans*-OCin-9), 7.56 (2H, m, *trans*-OCin-9), 7.38 (2H, m, *trans*-OCin-9), 7.37 (1H, m, *trans*-OCin-9), 6.80 (1H, q, *J* = 6.5 Hz, OTig-14), 6.38 (1H, d, *J* = 15.9 Hz, *trans*-OCin-9), 4.44 (1H, d, *J* = 16.1 Hz, OAcAc-1), 4.31 (1H, d, *J* = 16.1 Hz, OAcAc-1), 2.25 (3H, s, OAc-11), 2.12 (3H, s, OAc-6), 1.87 (3H, s, OAcAc-1), 1.79 (3H, s, OTig-14), 1.78 (3H, d, *J* = 6.5 Hz, OTig-14); <sup>13</sup>C NMR (CDCl<sub>3</sub>, 150 MHz) see Table 3 and  $\delta_{\text{C}}$  170.4 (C, OAc-11), 170.2 (C, OAc-6), 169.9 (C, OAcAc-1), 167.2 (C, OTig-14), 166.7 (C, OAcAc-1), 165.6 (C, *trans*-OCin-9), 146.6 (CH, *trans*-OCin-9), 137.7 (CH, OTig-14), 134.3 (C, *trans*-OCin-9), 130.5 (CH, *trans*-OCin-9), 128.8 (CH, *trans*-OCin-9), 128.6 (CH, *trans*-OCin-9), 128.2 (C, OTig-14), 117.5 (CH, *trans*-OCin-9), 60.6 (CH<sub>2</sub>, OAcAc-1), 21.5 (CH<sub>3</sub>, OAc-6), 21.2 (CH<sub>3</sub>, OAc-11), 20.1 (CH<sub>3</sub>, OAcAc-1), 14.5 (CH<sub>3</sub>, OTig-14), 12.0 (CH<sub>3</sub>, OTig-14); (+)-LRESIMS *m/z* 715 (100) [M + H]<sup>+</sup>, 737 (40) [M + Na]<sup>+</sup>; (+)-HRESIMS *m/z* 737.2786 [M + Na]<sup>+</sup> (calcd for C<sub>37</sub>H<sub>46</sub>O<sub>14</sub>Na, 737.2780).

**X-ray Crystallography Analysis.** Colorless crystals of denhaminol A (1) were obtained by crystallization from acetone. Unique data sets for 1 as the acetone solvate were measured at 173 K on an Oxford-Diffraction GEMINI S Ultra CCD diffractometer with Cu K $\alpha$  radiation utilizing CrysAlis software.<sup>29</sup> The structure was solved by the direct methods package SIR97<sup>30</sup> and refined by full matrix least-squares refinement on *F*<sup>2</sup> using the WinGX software package<sup>31</sup> incorporating SHELXL.<sup>32</sup> Anisotropic thermal parameters were refined for non-hydrogen atoms; (*x*, *y*, *z*, *U*<sub>iso</sub>)<sub>H</sub> were included and constrained at estimated values. Conventional residuals at convergence are quoted; statistical weights were employed. The absolute configuration of 1 was determined by anomalous dispersion effects (2735 Bijvoet pairs, Flack parameter 0.10(11)).<sup>18</sup> ORTEP-3<sup>31</sup> and PLATON<sup>33</sup> software were utilized to prepare material for publication. Full .cif deposition resides with the Cambridge Crystallographic Data Centre (CCDC No. 1001309). Copies can be obtained free of charge on application at the following address: <http://www.ccdc.cam.ac.uk/cgi-bin/catre.cgi>.

**X-ray data for denhaminol A (1) acetone solvate:** C<sub>30</sub>H<sub>38</sub>O<sub>10</sub>·C<sub>3</sub>H<sub>6</sub>O, MW = 616.7; orthorhombic, space group *P*<sub>2</sub><sub>1</sub><sub>2</sub><sub>1</sub><sub>2</sub>, *a* = 8.8605(4), *b* = 16.2937(8), *c* = 22.6352(11) Å, *V* = 3267.9(3) Å<sup>3</sup>. *D*<sub>calc</sub> (*Z* = 4) = 1.25 g cm<sup>-3</sup>.  $\mu_{\text{Cu}}$  = 0.78 mm<sup>-1</sup>; crystal size 0.22 × 0.19 × 0.11 mm; *T*<sub>min/max</sub> = 0.848/0.919. 2 $\theta_{\max}$  = 71.6°; *N*<sub>t</sub> = 20086, *N* = 6296

(*R*<sub>int</sub> = 0.045), *N*<sub>0</sub> (*I* > 2 $\sigma$ (*I*)) = 5454; *R*<sub>1</sub> = 0.039, *wR*<sub>2</sub> = 0.108; *S* = 1.09,  $\kappa_{\text{abs}}$  = 0.10(11).

**AlamarBlue and Live-Cell Imaging Assays.** LNCaP cells were obtained from the American Type Culture Collection (ATCC, Manassas, VA, USA). LNCaP cells were cultured in phenol-red-free RPMI-1640 medium (Thermo Fisher Scientific) supplemented with 5% FBS (Thermo Fisher Scientific) at 37 °C in an atmosphere containing 5% CO<sub>2</sub> and maintained in log phase growth. Cell viability as a function of metabolic activity was measured by an AlamarBlue end point assay (Thermo Fisher Scientific) as previously described.<sup>22</sup> Briefly, LNCaP cells (4000 per well) were seeded for 24 h into 96-well tissue culture plates (Corning, Corning, NY, USA) and treated with the indicated compounds. Metabolic activity was measured with AlamarBlue according to the manufacturer's instructions (Thermo Fisher Scientific) after 72 h of treatment. Compounds were dissolved in DMSO and diluted in growth medium; the DMSO concentration in the medium did not exceed 0.4%. Control cells were treated with the equivalent dose of DMSO (negative control) or doxorubicin (Sigma-Aldrich, IC<sub>50</sub> = 36.1 ± 3.3 nM) as positive control. For live-cell imaging, cells were seeded and treated as above. As described before,<sup>24</sup> the 96-well plates were loaded into an IncuCyte live-cell imaging system (Essen BioScience, Ann Arbor, MI, USA), cells were imaged every 2 h for 96 h, and growth was measured as a function of increasing confluence. Calculations of half-maximal inhibitory concentration (IC<sub>50</sub>) after 72 h of treatment were performed with GraphPad Prism (GraphPad Software). Each data point was performed in triplicate and repeated in three independent experiments.

**Lipid Content Analysis.** The fluorescence intensity of the lipophilic staining reagent Nile Red is linearly correlated with the cellular lipid content.<sup>34</sup> Depending on the hydrophobicity of the bound lipids, Nile Red displays different fluorescent emission maxima.<sup>35</sup> For example, Nile Red-stained neutral lipids such as triacylglycerols and cholesterol esters, which are mainly stored in lipid droplets, fluoresce with an emission maximum of ~560 nm when excited at 485 nm. Nile Red-labeled polar lipids such as phosphatidylcholine, phosphatidylethanolamine, and phosphatidylserine, which are the main constituents of lipid bilayers, have an emission maximum at ~620 nm. Optical 96-well plates (ibidi, Martinsried, Germany) were coated with 100  $\mu$ L of poly-L-ornithine (Sigma-Aldrich) as described previously.<sup>36</sup> LNCaP cells were seeded at 3000 cells per well in phenol-red-free RPMI-1640 medium supplemented with 5% FBS for 48 h (Thermo Fisher Scientific). After 72 h of treatment, the medium was removed, and cells were fixed in 4% paraformaldehyde for 20 min on ice. Cells were then stained for 20 min at room temperature in the dark in 150  $\mu$ L of PBS containing 1.0  $\mu$ g/mL DAPI [2-(4-aminophenyl)-1*H*-indole-6-carboxamide, Sigma-Aldrich] and 0.25  $\mu$ g/mL Nile Red (Sigma-Aldrich). Images were acquired on a Cytell Cell Imaging System (GE Healthcare, Little Chalfont, UK) using the DAPI, Cy3, and Cy5 channels at a 10 $\times$  magnification. Image segmentation and quantitation of cellular mean fluorescence intensities of phospholipids (Cy5) and neutral lipids (Cy3) of ~300 cells per treatment were performed with CellProfiler software (Broad Institute, Cambridge, MA, USA). Statistical significance was analyzed with GraphPad Prism by one-way ANOVA with Dunnett's multiple comparison test. Control cells were treated with the equivalent dose of DMSO (negative control) or TOFA (5-(tetradecyloxy)-2-furoic acid, Sigma-Aldrich) as positive control. Each data point was performed in duplicate and repeated in three independent experiments.

## ■ ASSOCIATED CONTENT

### Supporting Information

1D and 2D NMR spectra for denhaminols A–H (1–8) and LNCaP growth inhibition data at 100  $\mu$ M. This material is available free of charge via the Internet at <http://pubs.acs.org>.



## ■ AUTHOR INFORMATION

## Corresponding Author

\*Tel: +61-7-3735-6043. Fax: +61-7-3735-6001. E-mail: r.davis@griffith.edu.au.

## Notes

The authors declare no competing financial interest.

## ■ ACKNOWLEDGMENTS

The authors would like to thank R. White from Save Our Waterways Now (SOWN) for plant collection and identification. G. MacFarlane from the University of Queensland is acknowledged for HRESIMS measurements. C.L. would like to thank Griffith University for a Ph.D. scholarship (GUIPRS). The Australian Research Council is acknowledged for support toward the NMR and MS equipment (LE0668477 and LE0237908).

## ■ REFERENCES

- (1) McNeely, J. A.; Miller, K. R.; Reid, W. V.; Mittermeier, R. A.; Werner, T. B. *Conserving The World's Biological Diversity*; International Union for Conservation of Nature and Natural Resources, World Resources Institute, Conservation International, World Wildlife Fund-US and the World Bank: Gland, Switzerland, and Washington, D.C., 1990.
- (2) Williams, J.; Read, C.; Norton, A.; Dovers, S.; Burgman, M.; Proctor, W.; Anderson, H. *Biodiversity, Australia State of the Environment Report 2001 (Theme Report)*; CSIRO on behalf of the Department of the Environment and Heritage: Canberra, 2001.
- (3) The Royal Botanic Gardens & Domain Trust. PlantNET. <http://plantnet.rbgsyd.nsw.gov.au> (02-24-2014).
- (4) The Plant List (2013), Version 1.1. <http://www.theplantlist.org/1.1/browse/A/Celastraceae/> (02-24-2014).
- (5) Centre for Australian National Biodiversity Research, <http://www.anbg.gov.au/cpbr/cd-keys/rfk/index.html> (02-24-2014).
- (6) Grant, P. K.; Johnson, A. W. *J. Am. Chem. Soc.* **1957**, 4079–4089.
- (7) Inaba, Y.; Hasuda, T.; Hitotsuyanagi, Y.; Aoyagi, Y.; Fujikawa, N.; Onozaki, A.; Watanabe, A.; Kinoshita, T.; Takeya, K. *J. Nat. Prod.* **2013**, 76, 1085–1090.
- (8) Núñez, M. J.; Ardiles, A. E.; Martínez, M. L.; Torres-Romero, D.; Jiménez, I. A.; Bazzocchi, I. L. *Phytochem. Lett.* **2013**, 6, 148–151.
- (9) Descoins, C., Jr.; Bazzocchi, I. L.; Ravelo, A. G. *Chem. Pharm. Bull.* **2002**, 50, 199–202.
- (10) Gao, J. M.; Wu, W. J.; Zhang, J. W.; Konishi, Y. *Nat. Prod. Rep.* **2007**, 24, 1153–1589.
- (11) Brünig, R.; Wagner, H. *Phytochemistry* **1978**, 17, 1821–1858.
- (12) Wu, W.; Wang, M.; Zhu, J.; Zhou, W.; Hu, Z.; Ji, Z. *J. Nat. Prod.* **2001**, 64, 364–367.
- (13) Kuo, Y. H.; Chen, C. H.; Kuo, L. M.; King, M. L.; Wu, T. S.; Haruna, M.; Lee, K. H. *J. Nat. Prod.* **1990**, 53, 422–428.
- (14) Kim, S. E.; Kim, Y. H. C.; Lee, J. J. *J. Nat. Prod.* **1998**, 61, 108–111.
- (15) Torres-Romero, D.; Muñoz-Martínez, F.; Jiménez, I. A.; Castanys, S.; Gamarro, F.; Bazzocchi, I. L. *Org. Biomol. Chem.* **2009**, 7, 5166–5172.
- (16) Sang, H.; Wang, H.; Tu, Y.; Chen, Y. *Phytochemistry* **1991**, 30, 1547–1549.
- (17) Wang, Y.; Yang, L.; Tu, Y.; Zhang, K.; Chen, Y. *J. Nat. Prod.* **1997**, 60, 178–179.
- (18) Flack, H. D. *Acta Crystallogr. A* **1983**, 39, 876–881.
- (19) Numazawa, M.; Shlangouski, M.; Nakakoshi, M. *Steroids* **2001**, 66, 743–748.
- (20) Begley, M. J.; Crombie, L.; Crombie, W. M. L.; Toplis, D.; Whiting, D. A. *J. Chem. Soc., Perkin Trans. 1* **1990**, 2841–2846.
- (21) Joseph-Nathan, P.; Wesener, J. R.; Günther, H. *Magn. Reson. Chem.* **1984**, 22, 190–191.
- (22) Khokhar, S.; Feng, Y.; Campitelli, M. R.; Ekins, M. G.; Hooper, J. N. A.; Beattie, K. D.; Sadowski, M. C.; Nelson, C. C.; Davis, R. A. *Bioorg. Med. Chem. Lett.* **2014**, 24, 3329–3332.
- (23) Baron, P. S.; Neve, J. E.; Camp, D.; Suraweera, L.; Lam, A.; Lai, J.; Jovanovic, L.; Nelson, C.; Davis, R. A. *Magn. Reson. Chem.* **2013**, 51, 358–363.
- (24) Sadowski, M. C.; Pouwer, R. H.; Gunter, J. H.; Lubik, A. A.; Quinn, R. J.; Nelson, C. C. *Oncotarget* **2014**, 5, 9362–9381.
- (25) McCune, S. A.; Harris, R. A. *J. Biol. Chem.* **1979**, 254, 10095–10101.
- (26) Guseva, N. V.; Rokhlin, O. W.; Glover, R. A.; Cohen, M. B. *Cancer Biol. Ther.* **2011**, 12, 80–85.
- (27) Kridel, S. J.; Axelrod, F.; Rozenkrantz, N.; Smith, J. W. *Cancer Res.* **2004**, 64, 2070–2075.
- (28) Zhang, F.; Du, G. *World J. Biol. Chem.* **2012**, 3, 167–174.
- (29) Agilent Technologies. *CrysAlis Pro*; Yarton, Oxfordshire, UK, 2013.
- (30) Altomare, A.; Burla, M. C.; Camalli, M.; Cascarano, G. L.; Giacovazzo, C.; Guagliardi, A.; Moliterni, A. G. G.; Polidori, G.; Spagna, R. *J. Appl. Crystallogr.* **1999**, 32, 115–119.
- (31) Farrugia, L. *J. Appl. Crystallogr.* **2012**, 45, 849–854.
- (32) Sheldrick, G. M. *Acta Crystallogr. A* **2008**, 64, 112–122.
- (33) Spek, A. *J. Appl. Crystallogr.* **2003**, 36, 7–13.
- (34) Kwok, A. C. M.; Wong, J. T. Y. *Plant Cell Physiol.* **2005**, 46, 1973–1986.
- (35) Greenspan, P.; Mayer, E. P.; Fowler, S. D. *J. Cell. Biol.* **1985**, 100, 965–973.
- (36) Liberio, M. S.; Sadowski, M. C.; Soekmadji, C.; Davis, R. A.; Nelson, C. C. *PLoS One* **2014**, 9, e112122.